AIE-Active Photosensitizers

Subjects: Materials Science, Biomaterials

Contributor: Guan Wang, Xinggui Gu, Ben Zhong Tang

Photodynamic therapy (PDT) is a non-invasive approach for tumor elimination that is attracting more and more attention due to the advantages of minimal side effects and high precision. In typical PDT, reactive oxygen species (ROS) generated from photosensitizers play the pivotal role, determining the efficiency of PDT. However, applications of traditional PDT were usually limited by the aggregation-caused quenching (ACQ) effect of the photosensitizers employed. Fortunately, photosensitizers with aggregation-induced emission (AIE-active photosensitizers) have been developed with biocompatibility, effective ROS generation, and superior absorption, bringing about great interest for applications in oncotherapy.

Keywords: aggregation-induced emission ; photosensitizer ; reactive oxygen species

1. Introduction

Light has been used in the treatment of diseases for thousands of years. In ancient Egypt, *Ammi majus* Linnaeus was used to treat vitiligo, followed by exposing the patients to sunlight, and extracts from certain plants that contained photosensitizers were expanded to deal with other skin diseases. In the early 20th century, von Tappeiner discovered that photosensitizers could be used with light to kill cells, and defined this process as photodynamic therapy (PDT). Thereafter, the oxygen-dependence of PDT was revealed and the foundational principles of PDT were first described [1][2]. PDT became a special therapeutic strategy in treating patients, and the development of PDT as a non-invasive therapy flourished in the following decades.

PDT is generally implemented with the basic components of photosensitizers, light, and oxygen. Each component is basically non-toxic to the human body, and PDT can precisely control the killing of cancer cells and microorganisms by manipulating the wavelength, intensity, and irradiation range of light to reduce side effects in the treatment process, thereby boosting the development of antitumor treatments [3][4][5] and antibacterial applications [6][7][8].

The key factors for effective PDT applications are the reactive oxygen species (ROS) that originate from photosensitizers upon light irradiation. This process works by inducing tumor cell death by damaging the organelle and by suppressing cell proliferation by blocking the signaling pathway and inhibiting the cell cycle. Cell death caused by ROS has been well studied. As ROS are generated in cell, they can react with cellular components such as lipids, proteins, nucleic acids, and carbohydrates [9], leading to metabolic and cellular disturbances to achieve antitumor effects.

Accordingly, three main models of cell death caused by ROS in PDT, involving necrosis, apoptosis, and autophagy, are proposed [10][11]. Necrosis is a kind of passive cell death caused by ROS, and generally occurs as lipids and proteins in cellar membranes are subjected to damage by ROS, leading to the destruction of membrane integrity and ion homeostasis for the necrosis of cell. Apoptosis of cells in PDT is a programmed pathway triggered by initial damage to the organelles by ROS. It generally occurs as the signaling pathways from a cell's surface or from a site of cell damage are converged into a small number of central pathways, resulting in the final "execution" of the whole cell, followed by morphological changes in the cell [12]. Autophagy is a catabolic process that plays a pivotal role in renewing damaged organelles in cytoplasm, a mechanism that is considered important for cytoprotection. However, autophagy can also be stimulated by ROS, depending on the type of ROS and the degree of oxidative injury; alternatively, autophagy may occur abnormally by the destruction of organelles by ROS, eventually inducing cell death [11].

Generally, the response of cells to damage depends on several factors, such as the photosensitizer selected, the light dose applied, and the cellular metabolic state. The photosensitizer that is employed plays a critical role in the entire PDT process. Previously, many photosensitizers that involved inorganic and organic materials were developed and implemented for PDT. However, for purposes of biocompatibility and tunable photosensitization, organic photosensitizers exhibit superiority over other photosensitizers. Some examples of organic photosensitizers are provided in **Figure 1**.

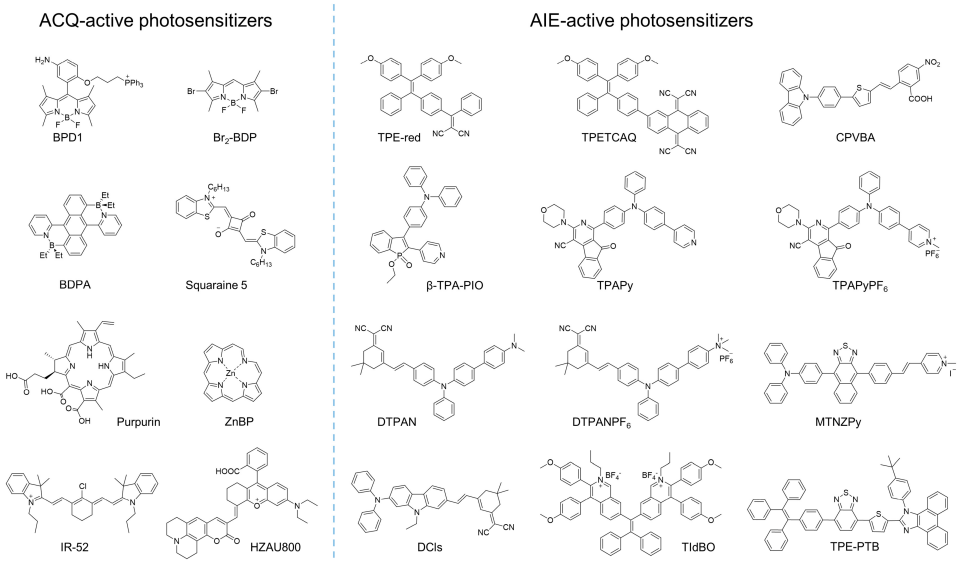

Figure 1. Examples of molecular structures of ACQ or AIE-active photosensitizers.

With the development of organic photosensitizers in recent decades, the photosensitization mechanism has been well-studied. The general photosensitization mechanism a photosensitizer is illustrated in the Jablonski diagram, as shown in **Figure 2** [13]. Upon absorbing a photon, the photosensitizer is excited into a higher-energy state from the singlet ground state (S_0), depending on the excitation wavelength, and it relaxes to the lowest excited single state (S_1) for the subsequent photophysical processes, according to Kasha's rule [14]. Although the excited molecule always undergoes an $S_1 \rightarrow S_0$ transition by releasing energy through a nonradiative pathway to yield heat or via radiative decay to produce fluorescence, it could also be transferred into the lowest excited triplet state (T_1) via $S_1 \rightarrow T_1$ intersystem crossing (ISC) processes, if the energy difference between S_1 and T_1 (ΔE_{ST}) is small enough or if their spin orbit coupling (SOC) effect is strong. Compared with the S_1 state, the high-energy T_1 exhibits a longer lifetime due to the prevention of spin in $T_1 \rightarrow S_0$, resulting in phosphorescence emission and possible ROS production.

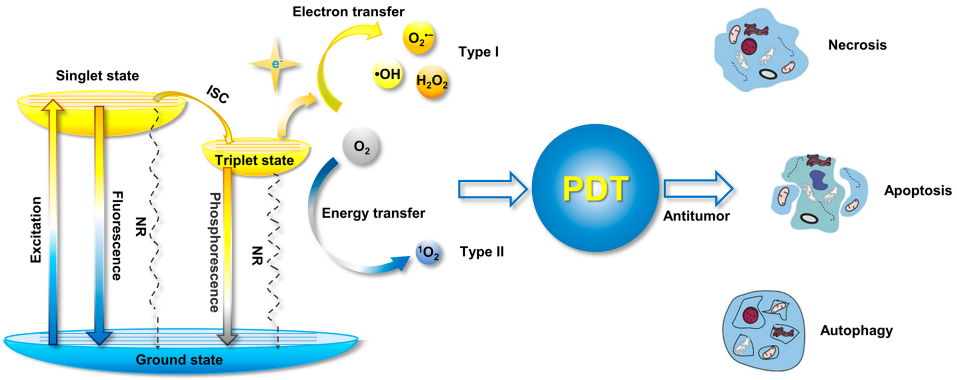

Figure 2. Mechanism of ROS generation form photosensitizer illustrated by Jablonski diagram, and the processes for PDT-induced cell death (NR: nonradiative pathway). Modified with the permission from the authors of [3]. Copyright 2020, the Author(s). Published by Elsevier.

According to the pathway of ROS generation, the obtained ROS could be classified in one of two types, type I and type II. Generally, type II ROS of singlet oxygen ($^1O_2$) could be harvested from the excited triplet state via energy transfer, covering the most commonly used organic photosensitizers, while type I ROS, including superoxide anion ($O_2^{\bullet-}$), hydroxyl radical (•OH), and hydrogen peroxide (H_2O_2) etc., are commonly obtained via a one-electron oxidation–reduction reaction with a neighboring oxygen molecule through electron transfer from an excited triplet state, which is more efficient for oxygen utilization and is usually considered to solve anoxia in the tumor microenvironment during PDT.

Although PDT has been implemented in the treatment of disease for a long time, the first organic photosensitizers were developed in the 1970s, and were considered to be the typical first-generation photosensitizers. They included a hematoporphyrin derivative (HpD) (containing a proprietary mix of porphyrin monomers, dimers, and oligomers) with porfimer sodium (the active material in HpD). Although they were the earliest and most useful photosensitizers in clinical trials, these photosensitizers suffered from relatively weak absorption of light, especially infrared or near-infrared (NIR) absorption. Such defects, as well as the unknown structures of the first-generation photosensitizers, hindered further applications, and encouraged the development of second-generation photosensitizers. Porphyrinoid compounds

comprising porphyrin or porphyrin-based macrocyclic analogues (such aschlorins and bacteriochlorins) and nonporphyrinoid compounds (anthraquinones, phenothiazines, and curcuminoids) with identified chemical structures were the second-generation photosensitizers [15]. These photosensitizers usually exhibited expanded absorption with wavelengths longer than 630 nm, as well as high extinction coefficients. Compared to the first-generation photosensitizers, the second-generation photosensitizers presented higher quantum yields of $^1O_2$, a higher tumor-to-normal tissue ratio, and, accordingly, a better antitumor effect. However, due to their hydrophobicity and lack of targeting, the applications of second-generation photosensitizers were also greatly limited. Many researchers in the field focused on developing third-generation photosensitizers with infrared absorption, better tumor specificity, and higher ROS generation.

In order to improve the efficiency of PDT, it is important to design photosensitizers that enhance ROS production. According to the mechanism of photosensitization, ROS are commonly generated from the excited triplet state via energy or electron transfer to surrounding oxygen molecules. Many strategies have been proposed to boost ROS generation, in which aggregation is one of the strategies for developing the photosensitizers required by promoting intersystem crossing (ISC) [16]. With appropriate aggregation, the enhanced photosensitization capability of various traditional photosensitizers, such as the photosensitization of pentamethine indocyanine [17], phthalocyanine [1][18], and porphyrin [19], has been demonstrated. However, due to the hydrophobicity of traditional photosensitizers, they aggregate in physiological circumstances, with aggregation-caused quenching (ACQ) effects that make it difficult to enhance ROS generation via aggregation because of the strong π-π interaction in aggregates [5]. Although scientists have developed a number of strategies to balance the notorious ACQ effects and aggregation-enhanced ROS generation, such as molecular modification [20] and polymer isolation [21], most of these strategies relied heavily on complicated chemical syntheses or low concentrations of photosensitizers in the photodynamic agents.

Fortunately, the concept of aggregate-induced emission (AIE) was proposed in 2001 [22][23][24][25]. Luminogens with aggregation-induced emission characteristics (AIEgens) commonly emitted weakly in solution, while they would exhibit intense fluorescence as they aggregated (**Figure 3**a), overcoming the obstacle of ACQ as the dyes aggregated and providing new opportunities for constructing functional luminogens. To achieve insights into AIE, much effort was devoted by researchers, and the primary mechanism for interpreting the AIE phenomenon was widely regarded as the restriction of intramolecular motions (RIM), including the restriction of intramolecular rotations (RIR) and the restriction of intramolecular vibrations (RIV), as shown in **Figure 3**b. As the photosensitizers were designed with AIE characteristics, they could be utilized in a high concentration for pursuing effective PDT without the disadvantages of the ACQ effects. Therefore, photosensitizers with AIE characteristics have been well-studied, and numerous of AIE-active photosensitizers with effective ROS generation and infrared absorption have been developed, boosting the development of PDT. A number of reviews have been published to summarize the development of AIE-active photosensitizers and the subsequent PDT, which made it convenient for researchers in understanding the progress of related fields [26][27][28][29][30][31][32][33][34]. However, those reviews concentrated mostly on the applications of PDT, with less focus on the design of AIE-active photosensitizers and manipulation of ROS generation.

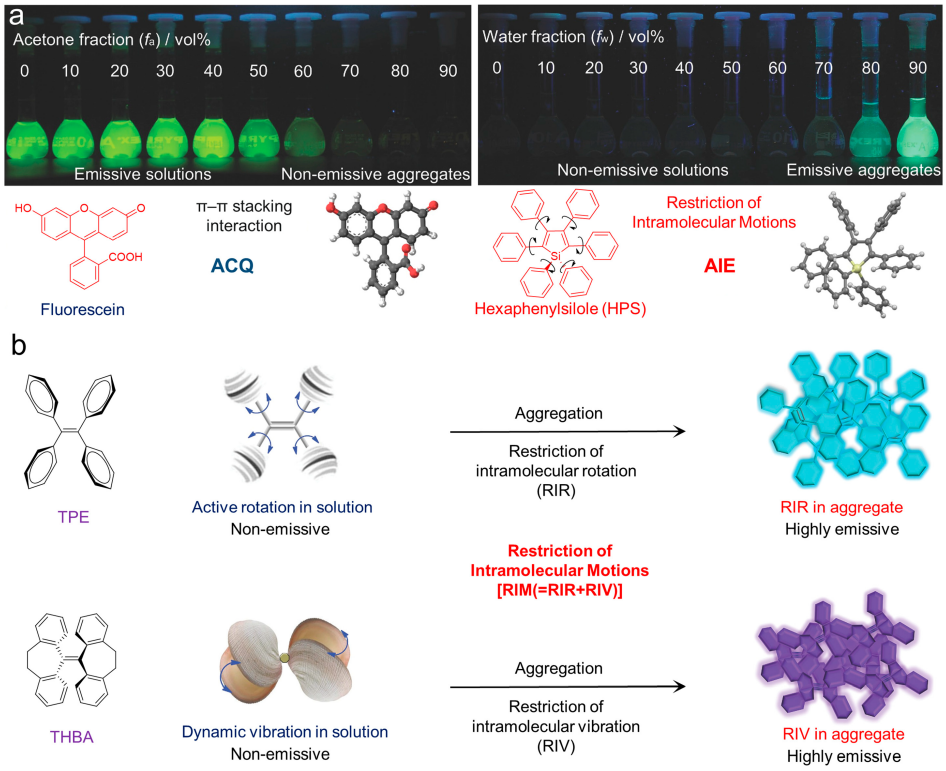

Figure 3. (**a**) Fluorescent photographs of the ACQ and AIE molecules as they aggregated in solution; (**b**) schematic illustration of the mechanisms of the ACQ and AIE phenomenon. Reprinted with the copyright from [24]. Copyright 2014, Wiley-VCH GmbH.

2. Advanced Development in PDT

Compared with traditional cancer treatment modalities, such as radiotherapy and chemotherapy, PDT exhibits the advantages of safety and non-invasiveness. Employing photosensitizers to generate ROS under a certain wavelength of light irradiation, PDT has been widely implemented in oncotherapy. However, the efficiency of PDT relies on the performance of the photosensitizers, and the development of the photosensitizers has dominated the improvement of PDT. The cutting-edge progress achieved by PDT based on the AIE-active photosensitizer, including NIR-absorbent PDT, activatable PDT, hypoxic PDT, and synergistic therapy.

2.1. Near Infrared Absorbent PDT

Compared to visible light, NIR light (700–1700 nm) demonstrated greater superiority based on reduced photodamage, lower scattering, and deeper light penetration [35][36]. Therefore, photosensitizers with both excitation and emission in the NIR regions are ideal candidates for PDT, and more and more studies were conducted to develop new NIR-absorbent photosensitizers. Tang et al. [37] prepared a series of molecules with far-red and NIR emission, good two-photon absorption, and efficient $^1O_2$ generation by modifying the electron-donating group of diphenylamine through an electron-rich carbazole ring with different electron-withdrawing groups (malononitrile, isophorone, methylpyridinium salt, and 3-cyano-4-phenyl-2(5H)-furanone), as shown in **Figure 4**a. Notably, DCMa (λ_{abs} = 478 nm, λ_{em} = 665 nm), DCIs (λ_{abs} = 510 nm, λ_{em} = 709 nm), and DCFu (λ_{abs} = 538 nm, λ_{em} = 755 nm) exhibited the ability to specifically target lipid droplets (LDs), while the cationic lipophilic DCPy (λ_{abs} = 454 nm, λ_{em} = 698 nm) was endowed with excellent mitochondrion-specific targeting ability. Upon cellular imaging, all molecules exhibited good biocompatibility and high contrast, as well as higher photostability than that of commercial probes. The efficient $^1O_2$ generation of these fluorophores (especially DCPy) under white light irradiation can be applied to effective PDT, demonstrating the potential of AIE-active photosensitizers as two-photon fluorescence-imaging agents for imaging-guided PDT. Similarly, as shown in **Figure 4**b, by encapsulating the AIE-active TPE-PTB (λ_{ex} = 488 nm, λ_{em} = 601 nm) within lipids, Tang et al. [38] prepared special nanoparticles with two-photon absorption, bright far-red emission, high quantum yield, and efficient $^1O_2$ and •OH release. The obtained nanoparticles exhibited a maximum two-photon absorption cross-section (δ) of 560 GM at NIR region with a quantum yield of 23%, demonstrating high-resolution deep (up to 505 μm) tumor-imaging capability as they accumulated at the tumor. In addition, the AIE nanoparticles demonstrated excellent PDT efficiency in high ROS generation, indicating their great potential as powerful and safe therapeutic agents for oncotherapy. In addition to the photosensitizers mentioned in the works listed here, various NIR-absorbent photosensitizers have been developed, which have become the cutting-edge area for AIE-active photosensitizers [39].

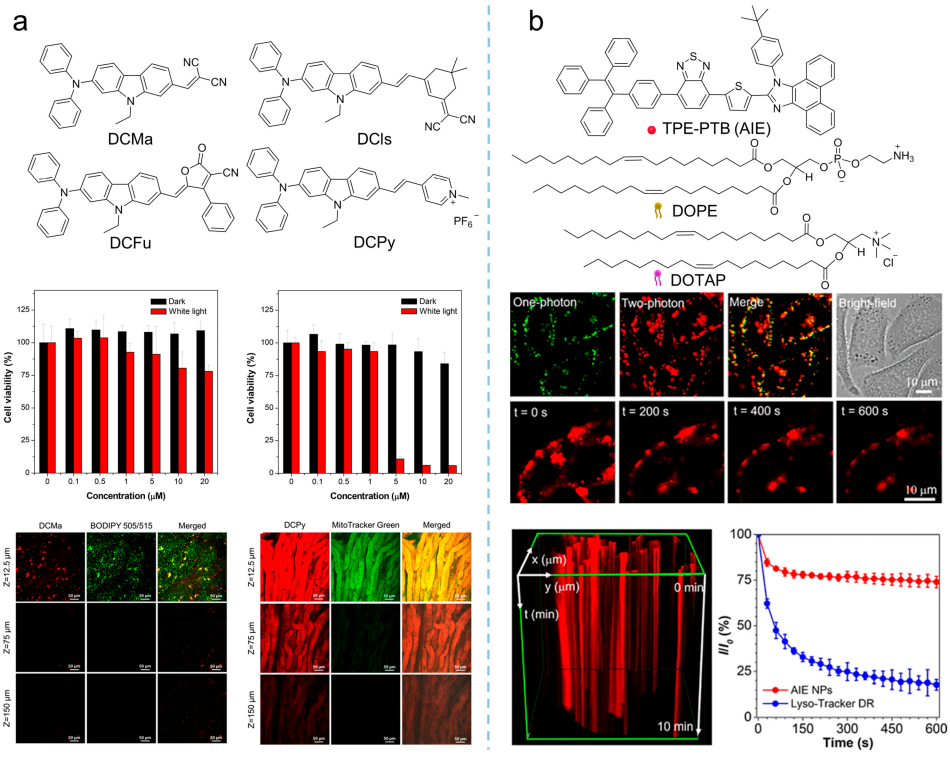

Figure 4. Multiphoton NIR absorption to enhance PDT theranostics. (**a**) Synthetic routes to DCMa, DCIs, DCFu, and DCPy and the in-vivo application of photosensitizers on the hepatic and nephric tissue of mice upon a 900 nm two-photon irradiation. Reprinted with the permission of the authors of [37]. Copyright 2018, American Chemical Society. (**b**) Molecular structure of TPE-PTB NPs, and cell imaging and photostability of AIE nanoparticles in A375 cells under continuous two-photon laser irradiation. Reprinted with the permission of the authors of [38]. Copyright 2020, American Chemical Society.

2.2. Activatable PDT

Designing activatable photosensitizers is an effective strategy for overcoming the uncontrolled phototoxicity of photosensitizers as they are implemented in vivo, providing smart oncotherapy for clinical applications. Owing to the rapid proliferation and vigorous metabolism of cancer cells, the tumor microenvironment always contains overexpressed factors, such as H_2O_2, GSH, hydrogen ion, and some enzymes, making it possible to construct activatable PDT [40][41][42]. As shown in **Figure 5**a, Liu et al. [43] synthesized an AIE-active photosensitizer (λ_{abs} = 480 nm, λ_{em} = 690 nm), followed by loading it into iron (III) carboxylate-based MOF, MIL-100 to produce PS@MIL-100. After that, a pH-sensitive doxorubicin (Dox)-PEG matrix was synthesized by Dox and PEG via a hydrazone bond. Using the self-assembly of Dox-PEG, PS@MIL-100 was encapsulated to prepare Dox-PEG-PS@MIL-100 nanoparticles. As the Dox-PEG-PS@MIL nanoparticles reached the tumor site, intertumoral H_2O_2 disorganized the nanoparticles and released the loaded photosensitizer on the tumor surface, and PDT was eventually triggered in the tumor.

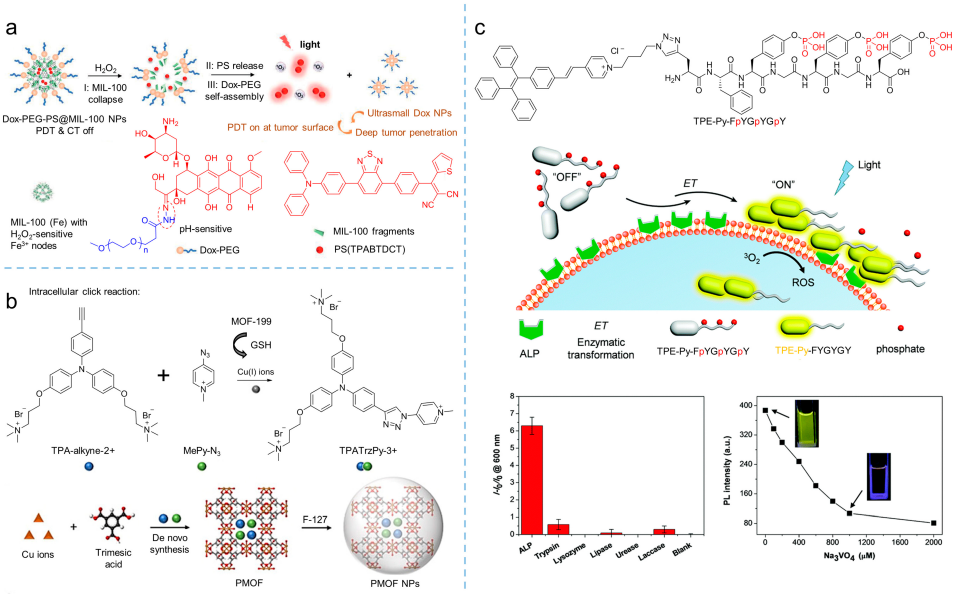

Figure 5. Activatable photosensitizers to enhance theranostics. (**a**) Schemes of MIL-100 collapse, PS release, and Dox-PEG self-assembly of Dox-PEG-PS@MIL-100 nanoparticles to tune PDT in H_2O_2. Reprinted with the permission of the authors of [43]. Copyright 2021, Wiley-VCH GmbH. (**b**) Scheme of the synthesis of TPATrzPy-3+ by two photochemically inert precursors under the catalysis of copper (I) ions generated from GSH-reduced-MOF-199. Reprinted with the permission of the authors of [44]. Copyright 2021, Wiley-VCH GmbH. (**c**) Schematic illustration of the self-assembly of TPE-Py-FpYGpYGpY under the catalysis of ALP, which significantly activates fluorescence and ROS generation. Reprinted with the permission of the authors of [45]. Copyright 2018, Royal Society of Chemistry.

GSH is considered as a reducing agent to balance intracell ROS production, and it maintains a high concentration due to vigorous metabolism, which is usually used to conduct activatable PDT. By introducing a GSH-activated click reaction, Liu et al. [44] developed an MOF-assisted activatable photosensitization system for targeted PDT. In their work, the Cu(II)-based metal-organic framework, MOF-199, was used as the carrier to load the reactants TPA-alkyne-2+ and MePy-N_3, and then encapsulated by F127 to obtain PMOF nanoparticles. The obtained nanoparticles were effectively enriched in the tumor and destroyed by GSH. As a result, the Cu(II) in the MOF was reduced into Cu(I), consequently releasing the reactants of TPA-alkyne-2+ and MePy-N_3. Catalyzed by Cu(I), the click reaction was initiated and the photosensitizer of TPATrzPy-3+ was obtained. Additionally, under light irradiation, mitochondrion-targeted TPATrzPy-3+ (λ_{ex} = 400 nm, λ_{em} = 595 nm) with an efficient generation of $^1O_2$ exhibited excellent PDT effectiveness.

Enzymes are another factor used for constructing activatable PDT. Recently, Ding et al. [45] synthesized the AIE-active photosensitizer of TPE-Py- FpYGpYGpY by modifying a short peptide with three tyrosine phosphates (pY). Due to the hydrophilic phosphotyrosine residue, the TPE-Py-FpYGpYGpY dissolved into water, resulting in weak fluorescence and negligible ROS generation. However, upon exposing TPE-Py-FpYGpYGpY in alkaline phosphatase (ALP) circumstances, an enzymatic cleavage of dephosphorylated precursors of TPE-Py-FpYGpYGpY was triggered, and the ALP-catalyzed

products were self-assembled, resulting in the ROS-active photosensitizer (λ_{ex} = 405 nm, λ_{em} = 600 nm), which demonstrated the potential of enzymatic-activated PDT.

2.3. Hypoxic PDT

Oxygen concentration in tumor tissue is varied, depending on tumor progression, angiogenesis, metabolism, and metastasis. However, hypoxia of the microenvironment is a characteristic feature of solid tumors. There is increasing evidence that PDT efficiency that relies on traditional photosensitizers is limited, due to the oxygen dependence of those photosensitizers [46]. Therefore, the development of therapeutic strategies to alleviate tumor hypoxia, including catalyzing intracellular substrates to produce oxygen and promoting ROS production through type I mechanism, have become the potential solutions. Qi et al. [47] synthesized the electron-rich MeOTPPM (λ_{abs} = 452 nm, λ_{em} = 667 nm) with a donor-acceptor structure, and proposed the concept of "more ICT effect in electron-rich anion-π^+ AIEgens, more effectively generate free radical ROS". Through their strategy, the synthesized MeOTPPM facilely generated type I ROS, exhibiting O_2 independence and an excellent PDT effect in a hypoxic microenvironment. In addition, MeOTPPM could specifically target mitochondria without the help of any additional targeted ligands, and its selective accumulation within cancer cells made it more PDT-efficient against cancer cells. Furthermore, Tang et al. [48] synthesized an electron-rich isoquinoline organic salt derivative, TIdBO, with excellent photoactivation properties, as shown in **Figure 6**a. The production of type I ROS from TIdBO could be significantly enhanced, due to the electron transfer during the photocyclization reaction. It is worth noting that the fluorescence intensity was enhanced after the ROS were produced and the apoptosis of cancer cells was subsequently triggered, realizing the self-monitoring of the PDT process.

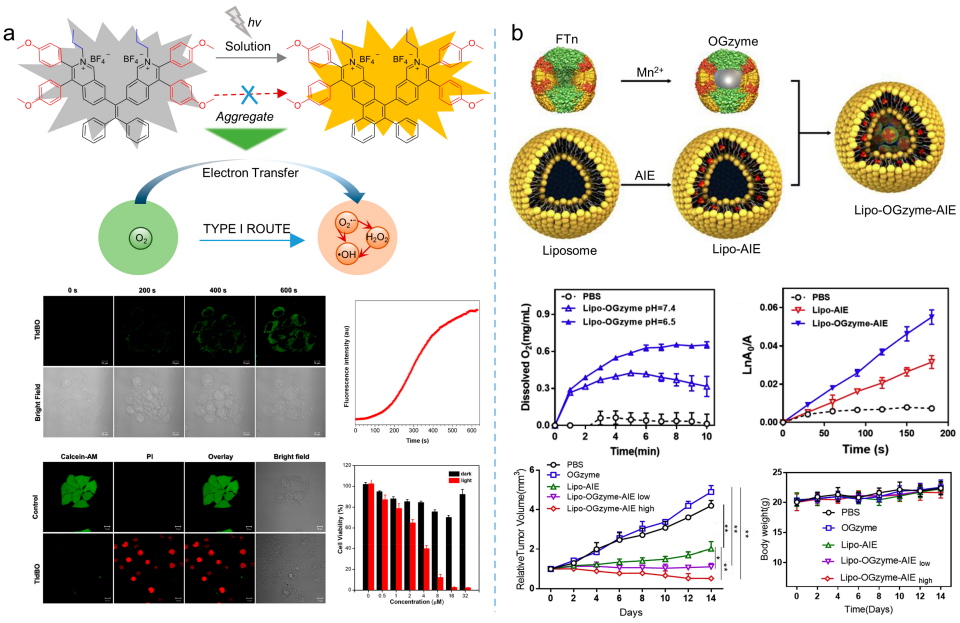

Figure 6. Type I ROS or self-oxygenated strategies to enhance theranostics. (**a**) Schematic illustration of producing type I ROS utilizing the electron transfer during the photoactivation process and theranostics effects of type I photosensitizers. Reprinted with the permission of the authors of [48]. Copyright 2021, American Chemical Society. (**b**) Schematic illustration of the preparation of nanoparticles, cascade reactions induced by the nanozymes and oxygen production, ROS production, and therapeutic effect of the nanozymes. Reprinted with the permission of the authors of [49]. Copyright 2020, Elsevier.

Except for producing type I ROS, strategies based on oxygen self-sufficient nanoplatform could be an alternative for overcoming hypoxic limitations. For example, as shown in **Figure 6**b, Huang et al. [49] prepared a hypoxia-tropic nanozyme as an oxygen generator (OGzyme) by the biomimetic synthesis of MnO_2 nanoparticles inside the hollow cavity of ferritin nanocages (FTn). After that, the obtained OGzyme and the AIE-active photosensitizer were encapsulated into phospholipid bilayers. As the OGzymes aggregated at the tumors' tissue, they provided sufficient oxygen for the photosensitization of an AIE-active photosensitizer by utilizing the H_2O_2 response of MnO_2. Hence, this system worked in hypoxic tumor tissue, and exhibited a strong PDT effect. Similarly, Liu et al. [50] developed carrier-free hybrid nanospheres comprising an AIE-active photosensitizer, iron ions, and a Bcl-2 inhibitor for hypoxic tumor PDT. Based on this strategy, the intracellular O_2 concentration was increased via a Fe^{3+}-derived Fenton reaction. Moreover, by inhibiting the production of Bcl-2 protein, intracellular ROS of the tumor was increased, and the PDT efficiency was improved synergistically.

2.4. Synergistic Therapy

The therapeutic efficiency of a single modality of PDT is often limited. It is crucial to develop a multifunctional treatment system for the synergistic therapy of tumors. Currently, the commonly used strategy for constructing multimodal optical therapeutic systems is a combination of multiple components in a single nanoplatform, such as synergistic photothermal therapy (PTT)/PDT and synergistic chemotherapy/PDT. As shown in **Figure 7**, by combining the positively charged and hydrophilic AIE-active photosensitizer (NH_2-PEG-TTPy) with the negatively charged surface black phosphorus nanosheets (BP nanosheets) via electrostatic interactions, Tang et al. [51] developed the nanomaterial of BP@PEG-TTPy (λ_{ex} = 488 nm, λ_{em} = 672 nm), which not only exhibited excellent stability, but also simultaneously integrated the advantages of the two components, including bright NIR fluorescence, efficient ROS generation, and the PTT effect. As a result, BP@PEG-TTPy achieves efficient imaging-guided PDT-PTT synergistic therapy under irradiation both in vitro and in vivo, demonstrating the significant improvement of synergistic therapy compared to that of single PDT.

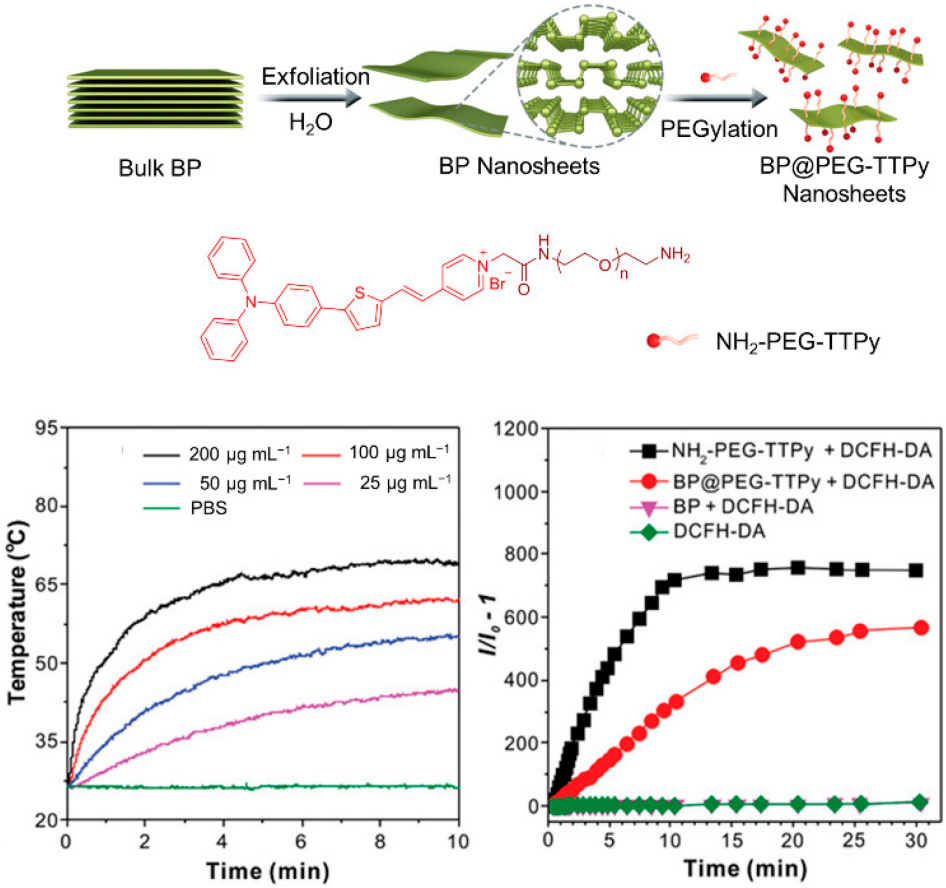

Figure 7. Synergistic therapy combining PDT. Schematic illustration of the preparation processes of BP@PEG-TTPy nanosheets and PDT/PTT effects of nanosheets. Reprinted with the permission of authors of [51]. Copyright 2020, Wiley-VCH GmbH.

Synergistic chemotherapy/PDT was also implemented in oncotherapy. Xia et al. [52] developed a reduction-sensitive co-delivery micelles TB@PMP for combinational therapy, where the chemotherapeutic drug, paclitaxel, was modified to the amphiphilic polymer through disulfide bonds, forming the reduction-sensitive polymer prodrug PMP, as shown in **Figure 8**a. The amphiphilic polymer prodrug PMP self-assembled into micelles in aqueous solution, and then encapsulated the AIE-active photosensitizer TPA-BDTO through a hydrophobic interaction. After that, TB@PMP (λ_{ex} = 530 nm, λ_{em} = 684 nm) micelles were passively enriched in the tumor site via the EPR effect. As the TB@PMP micelles were taken up by tumor cells, the disulfide bonds in PMP were cleaved, due to the high concentration of GSH in the tumor cells, resulting in the release of the paclitaxel. At the same time, TPA-BDTO produced cytotoxic ROS under light irradiation. As a result, when the ROS and the paclitaxel were combined, the balance between the microtubule aggregation and deaggregation was disrupted by the paclitaxel, which led to replication failure and, ultimately, the cancer cell apoptosis. Moreover, Singh et al. [53] prepared one-component organic nanoparticles for chemo-photodynamic therapy by conjugating a TPE moiety with a *p*-hydroxy phenacyl-chlorambucil conjugate. When exposed to visible light, the obtained nanoparticles simultaneously produced $^1O_2$ and released the anticancer drug chlorambucil. The cytotoxicity assay showed that the anticancer activity of the obtained nanoparticles was significantly enhanced by the synergistic combination therapy.

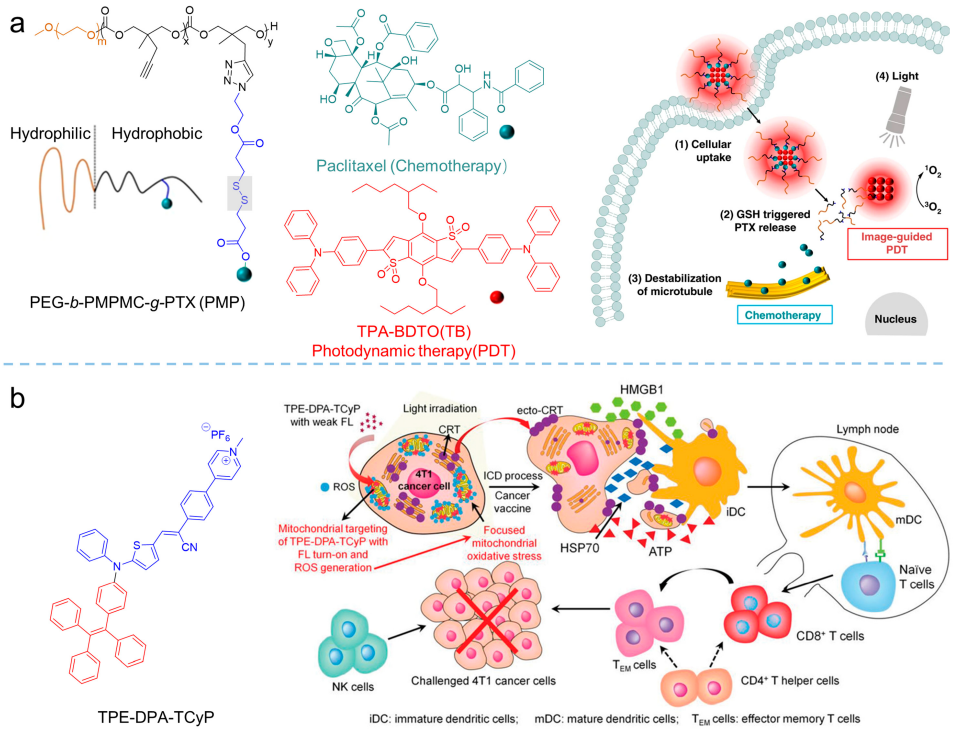

Figure 8. Synergistic therapy combining PDT. (**a**) Structure of the PEG-*b*-PMPMC-*g*-PTX (PMP) and TB@PMP (+), which was employed for combinational PDT/chemotherapy. Reprinted with the permission of the authors of [52]. Copyright 2018, by the author(s). Published by Springer Nature. (**b**) Schematic illustration of TPE-DPA-TCyP as an effective ICD inducer for antitumor immunity. Reprinted with the permission of the authors of [54]. Copyright 2019, Wiley-VCH GmbH.

A combination of PDT and immunotherapy has been emerging as a new strategy for cancer treatment [55]. In the processes of combined PDT and immunotherapy, calreticulin (CRT) would translocate to the cell membrane from the endoplasmic reticulum (ER) upon the stimuli of ROS, facilitated dendritic cell (DC) recruitment, recognition, and antigen presentation, to strengthen the host's immune response [56][57]. Based on that, Ding et al. [54] synthesized the AIE-active photosensitizer of TPE-DPA-TCyP (λ_{abs} = 504 nm, λ_{em} = 697 nm) with mitochondrial targeting. Employing the ROS generation of the TPE-DPA-TCyP, the mitochondrial oxidative stress rose and resulted in immunogenic cell death (ICD). In their work, the effective in vivo ICD immunogenicity of TPE-DPA-TCyP was demonstrated using a prophylactic tumor vaccination model, revealing that intracellular oxidative stress in mitochondria could also cause ICD, rather than the commonly accepted ICD that originated from ER. The comprehensive mechanism of TPE-DPA-TCyP in ICD processes was verified by immune cell analyses, which provided a highly effective strategy for evoking abundant and large-scale ICD. Additional related works have been reviewed by Li [26] and Ding [58].

References

1. Li, X.; Lee, D.; Huang, J.D.; Yoon, J. Phthalocyanine-Assembled Nanodots as Photosensitizers for Highly Efficient Type I Photoreactions in Photodynamic Therapy. Angew. Chem. Int. Ed. 2018, 57, 9885–9890.
2. Tappenier, H.V. Therapeutische versuche mit fluoreszierenden stoffen. Muench. Med. Wochenschr. 1903, 47, 2042–2044.
3. Sun, Y.; Zhao, D.; Wang, G.; Wang, Y.; Cao, L.; Sun, J.; Jiang, Q.; He, Z. Recent progress of hypoxia-modulated multifunctional nanomedicines to enhance photodynamic therapy: Opportunities, challenges, and future development. Acta Pharm. Sin. B 2020, 10, 1382–1396.
4. Chilakamarthi, U.; Giribabu, L. Photodynamic Therapy: Past, Present and Future. Chem. Rec. 2017, 17, 775–802.
5. Bonnett, R. Photosensitizers of the porphyrin and phthalocyanine series for photodynamic therapy. Chem. Soc. Rev. 1995, 24, 19–33.
6. Sun, J.; Hu, F.; Ma, Y.; Li, Y.; Wang, G.; Gu, X. AIE-based Systems for Imaging and Image-guided Killing of Pathogens. In Handbook of Aggregation-Induced Emission; Tang, Y., Tang, B.Z., Eds.; John Wiley & Sons Ltd.: Hoboken, NJ, USA, 2022; Volume 3, pp. 297–327.
7. Sobotta, L.; Skupin-Mrugalska, P.; Piskorz, J.; Mielcarek, J. Porphyrinoid photosensitizers mediated photodynamic inactivation against bacteria. Eur. J. Med. Chem. 2019, 175, 72–106.

8. Oyim, J.; Omolo, C.A.; Amuhaya, E.K. Photodynamic Antimicrobial Chemotherapy: Advancements in Porphyrin-Based Photosensitize Development. Front. Chem. 2021, 9, 635344.
9. Martínez-Cayuela, M. Oxygen free radicals and human disease. Biochimie 1995, 77, 147–161.
10. Plaetzer, K.; Kiesslich, T.; Verwanger, T.; Krammer, B. The Modes of Cell Death Induced by PDT: An Overview. Med. Laser Appl. 2003, 18, 7–19.
11. Mroz, P.; Yaroslavsky, A.; Kharkwal, G.B.; Hamblin, M.R. Cell Death Pathways in Photodynamic Therapy of Cancer. Cancers 2011, 3, 2516–2539.
12. Oleinick, N.L.; Morris, R.L.; Belichenko, I. The role of apoptosis in response to photodynamic therapy: What, where, why, and how. Photochem. Photobiol. Sci. 2002, 1, 1–21.
13. Wang, G.; Gu, X.; Tang, B.Z. Chapter 17 AIEgen-based photosensitizers for photodynamic therapy. In Aggregation-Induced Emission Applications in Biosensing, Bioimaging and Biomedicine; Gu, X., Tang, B.Z., Eds.; De Gruyter: Berlin, Germany, 2022; Volume 2, pp. 485–522.
14. Kasha, M. Energy Transfer Mechanisms and the Molecular Excition Model for Molecular Aggregates. Radiat. Res. 1963, 20, 55–70.
15. Ormond, A.B.; Freeman, H.S. Dye Sensitizers for Photodynamic Therapy. Materials 2013, 6, 817–840.
16. Yang, L.; Wang, X.; Zhang, G.; Chen, X.; Zhang, G.; Jiang, J. Aggregation-induced intersystem crossing: A novel strategy for efficient molecular phosphorescence. Nanoscale 2016, 8, 17422–17426.
17. Ji, C.; Gao, Q.; Dong, X.; Yin, W.; Gu, Z.; Gan, Z.; Zhao, Y.; Yin, M. A Size-Reducible Nanodrug with an Aggregation-Enhanced Photodynamic Effect for Deep Chemo-Photodynamic Therapy. Angew. Chem. Int. Ed. 2018, 57, 11384–11388.
18. Lee, E.; Li, X.S.; Oh, J.; Kwon, N.; Kim, G.; Kim, D.; Yoon, J. A boronic acid-functionalized phthalocyanine with an aggregation-enhanced photodynamic effect for combating antibiotic-resistant bacteria. Chem. Sci. 2020, 11, 5735–5739.
19. Hsieh, M.C.; Chien, C.H.; Chang, C.C.; Chang, T.C. Aggregation induced photodynamic therapy enhancement based on linear and nonlinear excited FRET of fluorescent organic nanoparticles. J. Mater. Chem. B 2013, 1, 2350–2357.
20. Uchoa, A.F.; de Oliveira, K.T.; Baptista, M.S.; Bortoluzzi, A.J.; Iamamoto, Y.; Serra, O.A. Chlorin Photosensitizers Sterically Designed To Prevent Self-Aggregation. J. Org. Chem. 2011, 76, 8824–8832.
21. Tada, D.B.; Baptista, M.S. Photosensitizing nanoparticles and the modulation of ROS generation. Front. Chem. 2015, 3, 33.
22. Luo, J.; Xie, Z.; Lam, J.W.Y.; Cheng, L.; Chen, H.; Qiu, C.; Kwok, H.S.; Zhan, X.; Liu, Y.; Zhu, D.; et al. Aggregation-induced emission of 1-methyl-1,2,3,4,5-pentaphenylsilole. Chem. Commun. 2001, 18, 1740–1741.
23. Hong, Y.; Lam, J.W.Y.; Tang, B.Z. Aggregation-induced emission. Chem. Soc. Rev. 2011, 40, 5361–5388.
24. Mei, J.; Hong, Y.; Lam, J.W.Y.; Qin, A.; Tang, Y.; Tang, B.Z. Aggregation-Induced Emission: The Whole Is More Brilliant than the Parts. Adv. Mater. 2014, 26, 5429–5479.
25. Mei, J.; Leung, N.L.C.; Kwok, R.T.K.; Lam, J.W.Y.; Tang, B.Z. Aggregation-Induced Emission: Together We Shine, United We Soar! Chem. Rev. 2015, 115, 11718–11940.
26. Zha, M.; Yang, G.; Li, Y.; Zhang, C.; Li, B.; Li, K. Recent Advances in AIEgen-Based Photodynamic Therapy and Immunotherapy. Adv. Healthc. Mater. 2021, 10, 2101066.
27. Wang, S.; Wang, X.; Yu, L.; Sun, M. Progress and trends of photodynamic therapy: From traditional photosensitizers to AIE-based photosensitizers. Photodiagn. Photodyn. Ther. 2021, 34, 102254.
28. Wang, L.; Hu, R.; Qin, A.; Tang, B.Z. Conjugated Polymers with Aggregation-Induced Emission Characteristics for Fluorescence Imaging and Photodynamic Therapy. Chemmedchem 2021, 16, 2330–2338.
29. Liu, S.; Feng, G.; Tang, B.Z.; Liu, B. Recent advances of AIE light-up probes for photodynamic therapy. Chem. Sci. 2021, 12, 6488–6506.
30. He, Z.; Tian, S.; Gao, Y.; Meng, F.; Luo, L. Luminescent AIE Dots for Anticancer Photodynamic Therapy. Front. Chem. 2021, 9, 672917.
31. Chen, H.; Wan, Y.; Cui, X.; Li, S.; Lee, C.S. Recent Advances in Hypoxia-Overcoming Strategy of Aggregation-Induced Emission Photosensitizers for Efficient Photodynamic Therapy. Adv. Healthc. Mater. 2021, 10, 210607.
32. Dai, J.; Wu, X.; Ding, S.; Lou, X.; Xia, F.; Wang, S.; Hong, Y. Aggregation-Induced Emission Photosensitizers: From Molecular Design to Photodynamic Therapy. J. Med. Chem. 2020, 63, 1996–2012.

33. Zhang, R.; Duan, Y.; Liu, B. Recent advances of AIE dots in NIR imaging and phototherapy. Nanoscale 2019, 11, 19241–19250.

34. Hu, F.; Xu, S.; Liu, B. Photosensitizers with Aggregation-Induced Emission: Materials and Biomedical Applications. Adv. Mater. 2018, 30, 1801350.

35. Tu, Y.; Zhao, Z.; Lam, J.W.Y.; Tang, B.Z. Aggregate Science: Much to Explore in the Meso World. Matter 2021, 4, 338–349.

36. Gu, B.; Wu, W.; Xu, G.; Feng, G.; Yin, F.; Chong, P.H.J.; Qu, J.; Yong, K.T.; Liu, B. Precise Two-Photon Photodynamic Therapy using an Efficient Photosensitizer with Aggregation-Induced Emission Characteristics. Adv. Mater. 2017, 29, 1701076.

37. Zheng, Z.; Zhang, T.; Liu, H.; Chen, Y.; Kwok, R.T.K.; Ma, C.; Zhang, P.; Sung, H.H.Y.; Williams, I.D.; Lam, J.W.Y.; et al. Bright Near-Infrared Aggregation-Induced Emission Luminogens with Strong Two-Photon Absorption, Excellent Organelle Specificity, and Efficient Photodynamic Therapy Potential. ACS Nano 2018, 12, 8145–8159.

38. Li, Y.; Tang, R.; Liu, X.; Gong, J.; Zhao, Z.; Sheng, Z.; Zhang, J.; Li, X.; Niu, G.; Kwok, R.T.K.; et al. Bright Aggregation-Induced Emission Nanoparticles for Two-Photon Imaging and Localized Compound Therapy of Cancers. ACS Nano 2020, 14, 16840–16853.

39. Wang, D.; Lee, M.M.S.; Shan, G.; Kwok, R.T.K.; Lam, J.W.Y.; Su, H.; Cai, Y.; Tang, B.Z. Highly Efficient Photosensitizers with Far-Red/Near-Infrared Aggregation-Induced Emission for In Vitro and In Vivo Cancer Theranostics. Adv. Mater. 2018, 30, 1802105.

40. Lovell, J.F.; Liu, T.W.B.; Chen, J.; Zheng, G. Activatable Photosensitizers for Imaging and Therapy. Chem. Rev. 2010, 110, 2839–2857.

41. Xiong, Y.; Xiao, C.; Li, Z.; Yang, X. Engineering nanomedicine for glutathione depletion-augmented cancer therapy. Chem. Soc. Rev. 2021, 50, 6013–6041.

42. Yang, N.; Xiao, W.; Song, X.; Wang, W.; Dong, X. Recent Advances in Tumor Microenvironment Hydrogen Peroxide-Responsive Materials for Cancer Photodynamic Therapy. Nano-Micro Lett. 2020, 12, 15.

43. Wang, Y.; Shi, L.; Wu, W.; Qi, G.; Zhu, X.; Liu, B. Tumor-Activated Photosensitization and Size Transformation of Nanodrugs. Adv. Funct. Mater. 2021, 31, 2010241.

44. Wang, Y.; Xu, S.; Shi, L.; Teh, C.; Qi, G.; Liu, B. Cancer-Cell-Activated in situ Synthesis of Mitochondria-Targeting AIE Photosensitizer for Precise Photodynamic Therapy. Angew. Chem. Int. Ed. 2021, 60, 14945–14953.

45. Ji, S.; Gao, H.; Mu, W.; Ni, X.; Yi, X.; Shen, J.; Liu, Q.; Bao, P.; Ding, D. Enzyme-instructed self-assembly leads to the activation of optical properties for selective fluorescence detection and photodynamic ablation of cancer cells. J. Mater. Chem. B 2018, 6, 2566–2573.

46. Dang, J.; He, H.; Chen, D.; Yin, L. Manipulating tumor hypoxia toward enhanced photodynamic therapy (PDT). Biomater. Sci. 2017, 5, 1500–1511.

47. Zhao, X.; Dai, Y.; Ma, F.; Misal, S.; Hasrat, K.; Zhu, H.; Qi, Z. Molecular engineering to accelerate cancer cell discrimination and boost AIE-active type I photosensitizer for photodynamic therapy under hypoxia. Chem. Eng. J. 2021, 410, 128133.

48. Chen, K.; He, P.; Wang, Z.; Tang, B.Z. A Feasible Strategy of Fabricating Type I Photosensitizer for Photodynamic Therapy in Cancer Cells and Pathogens. ACS Nano 2021, 15, 7735–7743.

49. Gao, F.; Wu, J.; Gao, H.; Hu, X.; Liu, L.; Midgley, A.C.; Liu, Q.; Sun, Z.; Liu, Y.; Ding, D.; et al. Hypoxia-tropic nanozymes as oxygen generators for tumor-favoring theranostics. Biomaterials 2020, 230, 119635.

50. Shi, L.; Hu, F.; Duan, Y.; Wu, W.; Dong, J.; Meng, X.; Zhu, X.; Liu, B. Hybrid Nanospheres to Overcome Hypoxia and Intrinsic Oxidative Resistance for Enhanced Photodynamic Therapy. ACS Nano 2020, 14, 2183–2190.

51. Huang, J.; He, B.; Zhang, Z.; Li, Y.; Kang, M.; Wang, Y.; Li, K.; Wang, D.; Tang, B.Z. Aggregation-Induced Emission Luminogens Married to 2D Black Phosphorus Nanosheets for Highly Efficient Multimodal Theranostics. Adv. Mater. 2020, 32, 2003382.

52. Yi, X.; Dai, J.; Han, Y.; Xu, M.; Zhang, X.; Zhen, S.; Zhao, Z.; Lou, X.; Xia, F. A high therapeutic efficacy of polymeric prodrug nano-assembly for a combination of photodynamic therapy and chemotherapy. Commun. Biol. 2018, 1, 202.

53. Parthiban, C.; Sen, D.; Singh, N.D.P. Visible-Light-Triggered Fluorescent Organic Nanoparticles for Chemo-Photodynamic Therapy with Real-Time Cellular Imaging. ACS Appl. Nano Mater. 2018, 1, 6281–6288.

54. Chen, C.; Ni, X.; Jia, S.; Liang, Y.; Wu, X.; Kong, D.; Ding, D. Massively Evoking Immunogenic Cell Death by Focused Mitochondrial Oxidative Stress using an AIE Luminogen with a Twisted Molecular Structure. Adv. Mater. 2019, 31, 1904914.

55. Wang, G.; Zhou, L.; Zhang, P.; Zhao, E.; Zhou, L.H.; Chen, D.; Sun, J.; Gu, X.; Yang, W.; Tang, B.Z. Fluorescence Self-Reporting Precipitation Polymerization Based on Aggregation-Induced Emission for Constructing Optical Nanoagents. Angew. Chem. Int. Ed. 2020, 59, 10122–10128.
56. Galluzzi, L.; Buqué, A.; Kepp, O.; Zitvogel, L.; Kroemer, G. Immunogenic cell death in cancer and infectious disease. Nat. Rev. Immunol. 2017, 17, 97–111.
57. Yang, W.; Zhang, F.; Deng, H.; Lin, L.; Wang, S.; Kang, F.; Yu, G.; Lau, J.; Tian, R.; Zhang, M.; et al. Smart Nanovesicle-Mediated Immunogenic Cell Death through Tumor Microenvironment Modulation for Effective Photodynamic Immunotherapy. ACS Nano 2020, 14, 620–631.
58. Li, J.; Ou, H.; Ding, D. Recent Progress in Boosted PDT Induced Immunogenic Cell Death for Tumor Immunotherapy. Chem. Res. Chin. Univ. 2021, 37, 83–89.